SUPPORTING INFORMATION

Discovery of a potent dual inhibitor of acetylcholinesterase and butyrylcholinesterase with antioxidant activity that alleviates Alzheimer-like pathology in old APP/PS1 mice

Elisabet Viayna,[1,▽] Nicolas Coquelle,[2,3▽] Monika Cieslikiewicz-Bouet,[4] Pedro Cisternas,[5] Carolina A. Oliva,[5] Elena Sánchez-López,[6,7] Miren Ettcheto,[7,8,9] Manuela Bartolini,[10] Angela De Simone,[11] Mattia Ricchini,[1] Marisa Rendina,[1] Mégane Pons,[4] Omidreza Firuzi,[12] Belén Pérez,[13] Luciano Saso,[14] Vincenza Andrisano,[15] Florian Nachon,[16] Xavier Brazzolotto,[16] Maria Luisa García,[6,7] Antoni Camins,[7,8] Israel Silman,[17] Ludovic Jean,[4] Nibaldo C. Inestrosa,[5,18] Jacques-Philippe Colletier,*[,2] Pierre-Yves Renard,*[,4] and Diego Muñoz-Torrero*[,1]*

[1] Laboratory of Medicinal Chemistry (CSIC Associated Unit), Faculty of Pharmacy and Food Sciences, and Institute of Biomedicine (IBUB), University of Barcelona, Av. Joan XXIII 27-31, E-08028, Barcelona, Spain

[2] Institut de Biologie Structurale, Université Grenoble Alpes, CEA, CNRS UMR 5075, F-38054 Grenoble, France

[3] Large Scale Structures Group, Institut Laue-Langevin, F-38042 Grenoble Cedex 9, France

[4] Normandie University, UNIROUEN, INSA Rouen, CNRS, COBRA (UMR 6014), 76000 Rouen, France

[5] Center of Aging and Regeneration UC (CARE-UC), Departamento de Biología Celular y Molecular, Facultad de Ciencias Biológicas, Pontificia Universidad Católica de Chile, Av. Libertador Bernardo O'Higgins 340, P.O. Box 114, 8331150-Santiago, Chile

[6] Department of Pharmacy, Pharmaceutical Technology and Physical Chemistry, Faculty of Pharmacy and Food Sciences, and Institute of Nanoscience and Nanotechnology (IN2UB), University of Barcelona, Av. Joan XXIII 27-31, E-08028, Barcelona, Spain

[7] Biomedical Research Networking Centre in Neurodegenerative Diseases (CIBERNED), Institute of Health Carlos III, E-28031, Madrid, Spain

[8] Department of Pharmacology, Toxicology and Therapeutic Chemistry, Faculty of Pharmacy and Food Sciences, and Institute of Neuroscience, University of Barcelona, Av. Joan XXIII 27-31, E-08028, Barcelona, Spain

[9] Department of Biochemistry and Biotechnology, Faculty of Medicine and Health Sciences, University Rovira i Virgili, E-4320, Reus, Spain

[10] Department of Pharmacy and Biotechnology, Alma Mater Studiorum University of Bologna, Via Belmeloro 6, I-40126, Bologna, Italy

[11] Department of Drug Science and Technology, University of Turin, I-10125 Torino, Italy

[12] Medicinal and Natural Products Chemistry Research Center, Shiraz University of Medical Sciences, PO Box 3288, 71345 Shiraz, Iran

[13] Department of Pharmacology, Therapeutics and Toxicology, Autonomous University of Barcelona, E-08193, Bellaterra, Barcelona, Spain

[14] Department of Physiology and Pharmacology "Vittorio Erspamer", Sapienza University of Rome, P.le Aldo Moro 5, 00185 Rome, Italy

[15] Department for Life Quality Studies, University of Bologna, Corso d'Augusto 237, I-47921-Rimini, Italy

[16] Département de Toxicologie et Risques Chimiques, Institut de Recherche Biomédicale des Armées BP73, 91993 Brétigny sur Orge, France

[17] Department of Neurobiology, Weizmann Institute of Science, 76100 Rehovot, Israel

[18] Centro de Excelencia en Biomedicina de Magallanes (CEBIMA), Universidad de Magallanes, 6200000 Punta Arenas, Chile

TABLE OF CONTENTS

Table S1. Data Collection and Refinement Statistics[a]

Compound	5b	5c	5d	5h	5f	5i	
Protein	*Tc*AChE	*Tc*AChE	*Tc*AChE	*Tc*AChE	*Tc*AChE	*Tc*AChE	hBChE
ESRF Beamline	ID30A-1	ID30A-1	ID29	ID23-2	ID23-2	ID30A-1	ID30A-3
Resolution range (Å)	46.2–1.78 (1.84–1.78)	50.0–2.10 (2.10–2.15)	45.8–2.00 (2.05–2.00)	50.0–1.89 (1.96–1.89)	50.0–2.55 (2.62–2.55)	46.0–1.86 (1.93–1.86)	50.0–2.94 (3.11–2.94)
Space group	P 21 21 21	P 21 21 21	P 21 21 21	P 21 21 21	P 21 21 21	P 31 2 1	P 21 21 21
Unit cell (Å)	91.9 106.8 150.7	92.4 106.9 151.5	91.9 105.7 150.7	92.0 106.5 150.7	92.0 106.9 151.5	112.8 112.8 136.8	73.9 79.3 228.7
(°)	90 90 90	90 90 90	90 90 90	90 90 90	90 90 90	90 90 120	90 90 90
Total reflections	778360 (73377)	491356 (34392)	437206 (30229)	389055 (40693)	161616 (11640)	248253 (26362)	123120 (13347)
Unique reflections	141589 (13240)	87818 (6450)	99278 (6971)	115995 (11815)	48442 (3569)	83186 (8635)	26966 (3621)
Multiplicity	5.5 (5.5)	5.6 (5.3)	4.4 (4.3)	3.4 (3.4)	3.3 (3.3)	3.0 (3.1)	4.6 (3.7)
Completeness (%)	99.6 (99.5)	99.7 (99.8)	99.1 (95.4)	97.6 (97.1)	98.2 (98.6)	98.0 (99.0)	91.5 (81.6)
Mean I/sigma(I)	13.2 (1.6)	18.3 (2.5)	8.9 (1.8)	10.21 (1.8)	10.1 (1.9)	13.9 (1.7)	9.1 (1.0)
Wilson B-factor	35.0	37.1	37.1	33.9	41.3	43.4	69.3
R-merge	6.9 (99.6)	7.2 (65.1)	9.4 (72.7)	7.2 (70.7)	10.5 (65.5)	3.9 (76.6)	14.3 (119.0)
R-meas	7.6 (110.0)	7.9 (72.3)	10.7 (82.7)	8.5 (83.5)	12.4 (78.3)	4.8 (92.8)	16.1 (135.5)
CC1/2	0.999 (0.776)	0.999 (0.916)	0.997 (0.817)	0.998 (0.807)	0.995 (0.783)	0.999 (0.770)	0.993(0.405)
Reflections used in refinement	141778 (14028)	83177 (8247)	48379 (4789)	113964 (11247)	48379 (4789)	83177 (8247)	26923 (2235)
Reflections used for R-free	7082 (705)	4158 (400)	2287 (222)	5701 (564)	2287 (222)	4158 (400)	1356 (123)
R-work	0.1821 (0.2875)	0.1767 (0.2955)	0.2079 (0.2697)	0.1902 (0.3174)	0.2012 (0.2634)	0.1767 (0.2955)	0.2255 (0.3438)
R-free	0.2097 (0.3256)	0.1969 (0.3143)	0.2622 (0.3287)	0.2227 (0.3595)	0.2615 (0.3362)	0.1969 (0.3143)	0.3010 (0.4049)
Number of non-hydrogen atoms	9872	4796	8848	9870	8886	4796	8508
Macromolecules	8633	4309	8566	8578	8566	4309	8466
Ligands	170	57	41	204	82	57	42
Protein residues	1064	532	1064	1063	1064	532	1054
RMS(bonds)	0.008	0.007	0.006	0.007	0.008	0.007	0.012

RMS(angles)	0.93	0.82	0.80	0.91	0.94	0.82	1.55
Ramachandran favored (%)	96.6	96.3	95.5	96.7	95.2	96.3	91
Ramachandran allowed (%)	3.3	3.7	4.4	3.2	4.6	3.7	7.3
Ramachandran outliers (%)	0.1	0	0.1	0.1	0.2	0	1.9
Rotamer outliers (%)	2.1	1.7	1.3	2.5	1.2	1.7	2.6
Clashscore	4.97	3.50	5.03	5.57	5.25	3.50	27.29
Average B-factor	32.80	41.29	38.05	32.22	37.87	41.29	76.30
Macromolecules	31.50	40.43	38.01	30.76	37.84	40.43	76.29
Ligands	45.90	45.69	45.71	46.57	47.47	45.69	77.56
Solvent	41.19	41.99	38.21	40.99	35.78	49.35	n.a

[a] Statistics for the highest-resolution shell are shown in parentheses.

Table S2. Interaction of the 12-HC Hybrids 5b, 5c, 5d, 5f, and 5h with *Tc*AChE and of the 9-HC Hybrid 5i with *Tc*AChE and hBChE[a]

Linker and capsaicin moieties[b]	**5b (chain B)**	**5c (chain B)**	**5d**	**5f (chain A)**	**5f (chain B)**	**5h**	**5i–*Tc*AChE**	**5i–hBChE**
Hydrophobic interactions	Asp72 Tyr334	Asp72 Tyr334 Tyr70	Asp72 Tyr334 Tyr70 Trp279 Ile487	Asp72 Tyr334 Tyr70	Asp72 Tyr334 Tyr70	Asp72 Tyr334 Ile289 Trp279	Tyr121 Phe290 Phe331 Trp279 Ala328	Tyr334
π-stacking (perpendicular)								
Capsaicin moiety	Trp279	Trp279						
Triazole ring							Phe290	
Hydrogen bonds								
Amide O	Tyr121(OH)	HOH194 / Tyr121(OH)	Tyr70(OH) HOH582	Tyr121(OH)	Tyr121 OH	Tyr70(OH) HOH151	Phe288(N) HOH202 / Phe331(O)	Asp70(OE1)
Amide N	HOH369 Tyr70(OH)	Tyr70(OH)	HOH583 / Tyr121(OH) HOH561	HOH126 / Tyr70(OH)	HOH Y / Tyr70(OH)			
Hydroxyl O	HOH890 / Tyr334(O)	HOH349 / Ser286(OH) HOH721	Gly335(O) HOH568	Phe331(O)	Gly335(O)	Phe284(O) Ser286(OH/N)		Asn68(OD1)
Ether O			Gln185(NE2) (alternate conformer A) Ser286(N) (alternate conformer B) HOH587				HOH151 / Tyr70(OH)	Asn68(ND2)
Triazolylbutyl	-	-	-	-	-	-	Phe288(N)	

Huprine moiety	*Tc*AChE	hBChE
Hydrophobic interactions	Trp84 Phe330 Trp432 Ile439 Tyr442	Trp82 Phe329 Trp231 Ala328 Phe398
π-stacking (parallel)	Trp84 (parallel stacking) Phe330 (parallel stacking)	Trp82 (T-stacking) Phe290 (T-stacking)
Hydrogen bonds	His440	His440 Ser198

[a] All the interactions were determined using the plip server (doi:// 10.1093/nar/gkv315). [b] When two chains are available in the asymmetric unit, values are reported for the chain in which the electron density for the compound is best defined.

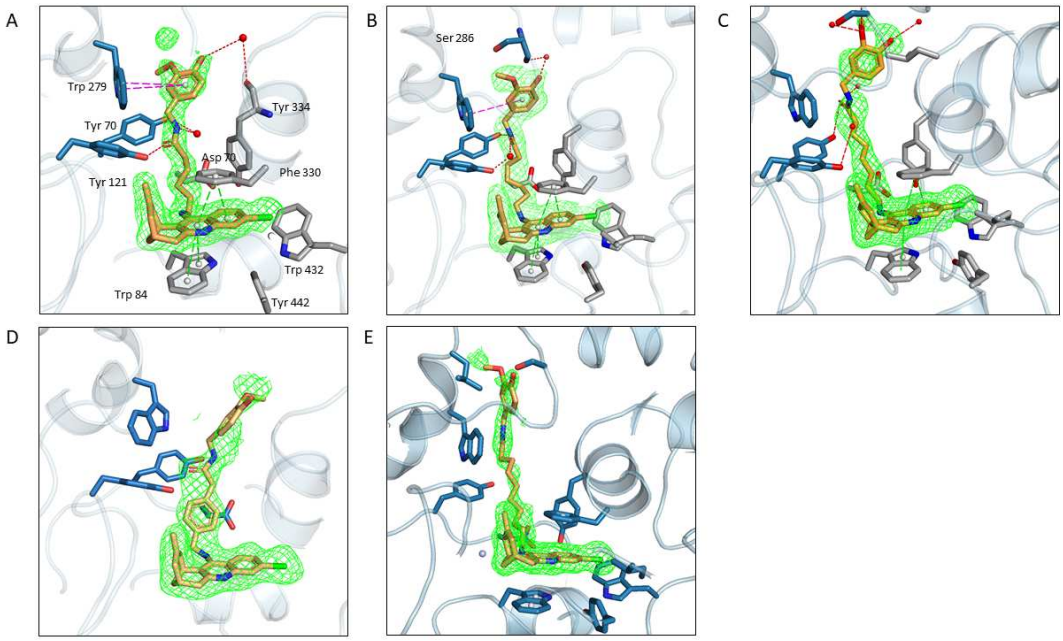

Figure S1. Polder maps have been computed for compounds **5b** (A), **5c** (B), **5d** (C), **5f** (D), and **5h** (E) in complex with *Tc*AChE. Maps have been contoured at 3 sigma.

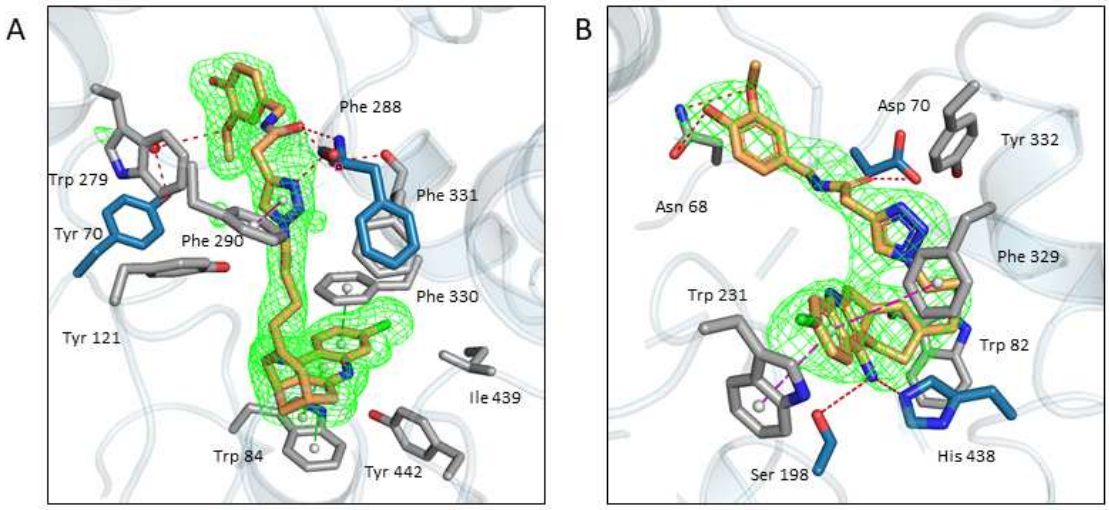

Figure S2. Polder maps have been computed for compound **5i** in complex with *Tc*AChE (A) and hBChE (B). Maps have been contoured at 4 sigma.

PAMPA-BBB Permeation Assay

Table S3. Literature and Experimental Permeability (*Pe* 10^{-6} cm s^{-1}) Values in the PAMPA-BBB Assay of the Commercial Drugs Used for Assay Validation.

Compound	**Bibliography value**[a]	**Experimental value (n=3) ± S.D.**
Cimetidine	0.0	0.7 ± 0.03
Norfloxacin	0.1	0.9 ± 0.02
Ofloxacin	0.8	1.0 ± 0.01
Lomefloxacin	1.1	0.7 ± 0.02
Hydrocortisone	1.9	1.4 ± 0.05
Piroxicam	2.5	1.7 ± 0.02
Costicosterone	5.1	6.7 ± 0.10
Clonidine	5.3	6.5 ± 0.05
Promazine	8.8	13.8 ± 0.3
Progesterone	9.3	16.8 ± 0.03
Desipramine	12	17.8 ± 0.10
Imipramine	13	12.3 ± 0.10
Verapamil	16	25.3 ± 0.78
Testosterone	17	24.0 ± 0.14

[a] From Di, L.; Kerns, E. H.; Fan, K.; McConnell, O. J.; Carter, G. T. High throughput artificial membrane permeability assay for blood-brain barrier. *Eur. J. Med. Chem.* **2003**, *38*, 223–232.

Table S4. Distribution of Hybrids 5c and 5i and the Reference Drug Donepezil to Different Organs and Plasma Levels[a]

	Distribution to tissues (µg compound / g of tissue)				Plasma levels (µg compound / mL)
compd	Brain	Kidneys	Liver	Lungs	
5c	1.58 ± 0.08	64.4 ± 47.5	112 ± 17	30.7 ± 0.40	< 0.003[b]
5i	18.9 ± 3.36	419 ± 62.5	227 ± 55	37.6 ± 0.53	0.036 ± 0.002
donepezil	6.13 ± 2.32	23.3 ± 0.4	14.8 ± 1.4	12.3 ± 5.23	6.46 ± 2.25

[a]Amounts measured 4 h after injection of the last dose of compound, at the end of a 2-week treatment period (2 mg/kg, ip, three times a week). Results are expressed as mean ± SD. [b]Detection limit.

Table S5. HPLC/MS/MS Gradient Method[a]

Time (min)	Flow	%A	%B
0	0.7	2.0	98.0
0.5	0.7	2.0	98.0
3.00	0.7	100	0
4	0.7	100	0
4.10	0.7	2.0	98.0
6	0.7	2.0	98.0

[a] Data were analyzed using one-way analysis of variance (ANOVA), followed by Tukey's post hoc test; * $p \leq 0.05$, ** $p \leq 0.01$, and *** $p \leq 0.001$ were considered significant differences. Statistical analyses were performed using Prism software (GraphPad, USA).

Table S6. Effects of 5i and 5c on Hippocampal β-Amyloid Levels[a]

	6 month-old APP/PS1 mice			11 month-old APP/PS1 mice		
	Aβ40 (pg/mL)	Aβ42 (pg/mL)	Aβ42/Aβ40 ratio	Aβ40 (pg/mL)	Aβ42 (pg/mL)	Aβ42/Aβ40
APP/PS1	8.32 ± 0.78	62.08 ± 4.43	7.52 ± 0.82	8.65 ± 0.44	69.04 ± 4.54	7.99 ± 0.60
APP/PS1 + **5i**	8.61 ± 1.02	58.54 ± 5.94	6.89 ± 1.09	18.42 ± 1.24	62.62 ± 3.68	3.42 ± 0.36
APP/PS1 + **5c**	7.25 ± 1.06	57.39 ± 2.72	8.07 ± 1.32	8.75 ± 1.33	65.86 ± 2.74	7.68 ± 1.27

[a] Hippocampal levels of Aβ40, Aβ42, and Aβ42/Aβ40 ratio in young and old male APP/PS1 mice treated with vehicle, **5i**, or **5c**. Data are expressed as mean values ± SEM of n = 7 animals in each group.

Additional information on "Figure 11. Synaptic transmission efficacy and plasticity mechanisms are affected in young APP/PS1 mice treated with compounds 5c and 5i"

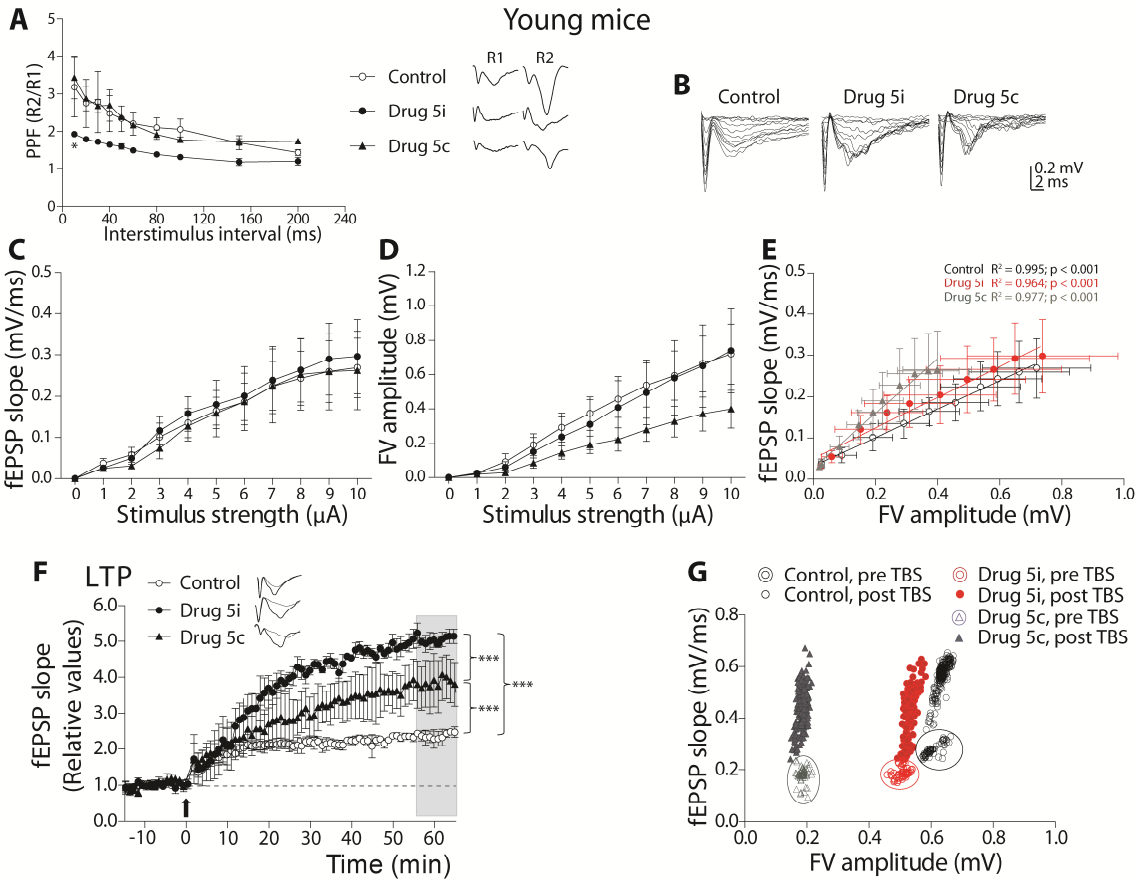

Figure 11E: We found a significant positive correlation between FV amplitude and fEPSP slopes in young mice, in control, Tg + **5c**, and Tg + **5i** groups [Tg control$_{slope}$ = 0.345 ± 0.008, R^2 = 0.995, $F_{(1,9)}$ = 1669, ***p < 0.001; Tg + **5i**$_{slope}$ = 0.375 ± 0.026, R^2 = 0.964, $F_{(1,9)}$ = 212.7, ***p < 0.001; Tg + **5c**$_{slope}$ = 0.667 ± 0.036, R^2 = 0.977, $F_{(1,9)}$ = 335.4, ***p < 0.001]. We also compared the linear regressions among groups using the analysis of covariance (ANCOVA). We found significant differences at intercepts between control and Tg + **5i** (ANCOVA: $F_{(1,17)}$ = 14.38, **p < 0.01), at intercepts between control and Tg + **5c** group (ANCOVA: $F_{(1,17)}$ = 22.69, ***p < 0.001), and at intercepts and slopes between Tg + **5i** and Tg + **5c** (ANCOVA intercepts: $F_{(1,17)}$ =

10.76, **p < 0.01, slope: $F_{(1,16)}$ = 37.34, ***p < 0.001). These data showed that control Tg mice had the lowest slope, which increased with both compounds.

Figure 11F: LTP induction, average of the last 10 min: one-way ANOVA, followed by Bonferroni's post-hoc test: Tg control vs Tg + **5i** ***p < 0.001; Tg control vs Tg + **5c**, ***p < 0.001; Tg + **5i** vs Tg + **5c**, ***p < 0.001.

Figure 11G: The range of FV amplitudes did not change before and after TBS, what ensures stability, but their values are different among groups (Tg control before TBS: 0.660 ± 0.002, after TBS: 0.652 ± 0.002 mV; Tg + **5i** before TBS: 0.503 ± 0.004, after TBS: 0.534 ± 0.002 mV; Tg + **5c** before TBS: 0.185 ± 0.001, after TBS: 0.185 ± 0.002 mV; one-way ANOVA ***p < 0.001, followed by Bonferroni's post-hoc test Tg control vs Tg + **5i** ***p < 0.001; Tg control vs Tg + **5c** ***p < 0.001; Tg + **5i** vs Tg + **5c** ***p < 0.001). To determine whether the strength between the FV amplitudes vs fEPSP slopes variables is significantly different between groups, we must compare correlation coefficients using Fisher 'r' to 'z' transformation. To do this, we first found the Pearson's correlation to obtain the correlation coefficient 'r' of each group, before the induction of LTP (Tg control: r = 0.803; Tg + **5i**: r = 0.553; Tg + **5c**: r = 0.112). Then, we used Fisher 'r' to 'z' transformation to compute how different were two correlation coefficients using the 'z' scores of each group (Tg control vs Tg + **5i**: z = 2.65, two-tailed p = 0.008; Tg control vs Tg + **5c**: z = 5.58, two-tailed p = 0; Tg + **5i** vs Tg + **5c**: z = 2.79, two-tailed p = 0.005). The positive 'z' indicates that the 'r' of the first group is larger than the one to which is compared. In our experiments, we obtained positive 'z' for all comparisons, and the correlations are statistically significant. We performed the same analysis to obtain the correlation coefficient 'r' of each group after the induction of LTP (Tg control: r = 0.876; Tg + **5i**: r = 0.722; Tg + **5c**: r = 0.521). Then, we obtained the 'z' scores of each group (Tg control vs Tg + **5i**: z = 4.96, two-tailed p = 0;

Tg control vs Tg + **5c**: z = 8.67, two-tailed p = 0; Tg + **5i** vs Tg + **5c**: z = 3.71, two-tailed p = 0.0002).

Additional information on "Figure 12. Synaptic transmission efficacy but not plasticity mechanisms are affected in old APP/PS1 mice treated with compounds 5i and 5c"

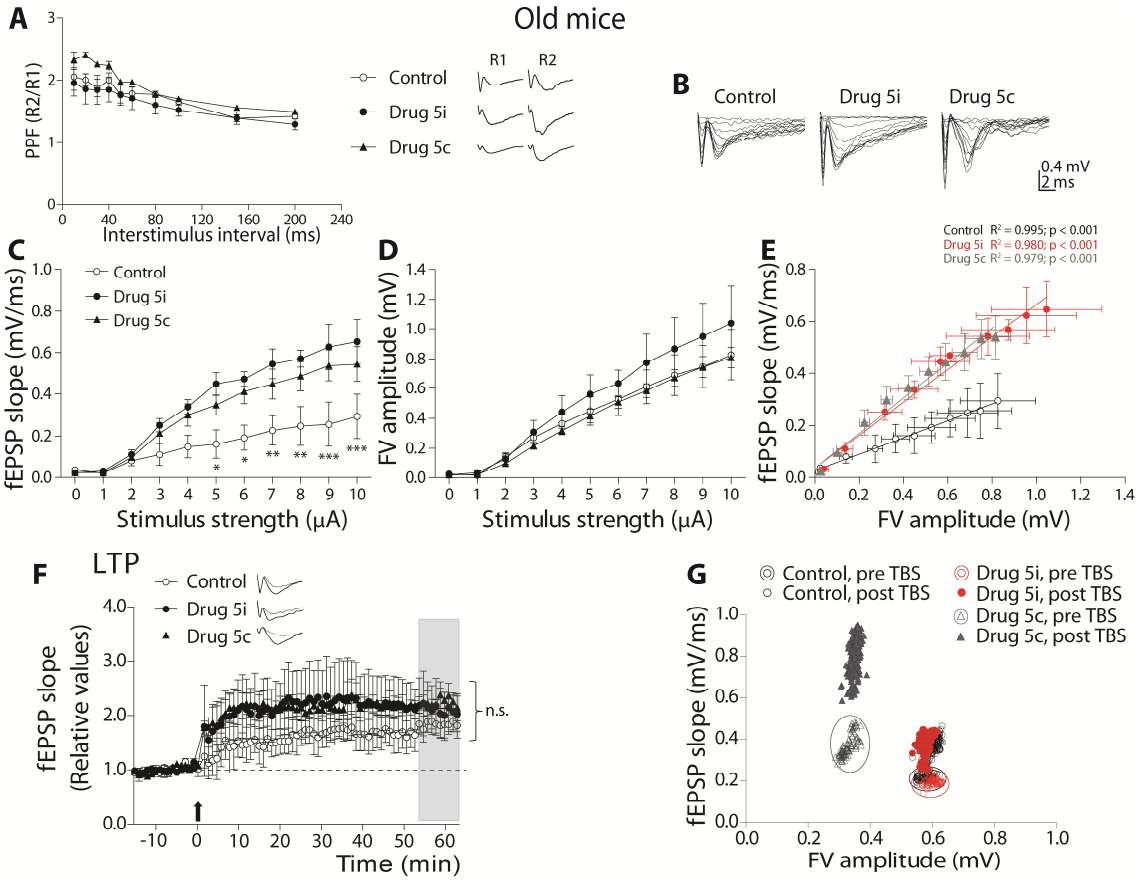

Figure 12C: Analysis by two-way ANOVA: interaction: $F_{(20,132)}$ = 1.56, p > 0.093; treatment: $F_{(2,132)}$ = 34.81, p < 0.001; stimulus amplitude: $F_{(10,132)}$ = 24.83, p < 0.001; Bonferroni's post-hoc test: Tg control vs Tg + **5i** at 5 and 6 µA, *p < 0.05; at 7 and 8 µA, **p < 0.01; at 9 and 10 µA, ***p < 0.001; Tg control vs Tg + **5c**, p > 0.05; Tg + **5i** vs Tg + **5c**, p = 0.097)

Figure 12E: We found a significant positive correlation between FV amplitude and fEPSP slopes in old mice, in control, Tg + **5c**, and Tg + **5i** groups (Tg $control_{slope}$ =

0.320 ± 0.008, R^2 = 0.995, $F_{(1,9)}$ = 1638, p < 0.001; Tg + **5i**$_{slope}$ = 0.636 ± 0.030, R^2 = 0.980, $F_{(1,9)}$ = 448.6, p < 0.001; Tg + **5c**$_{slope}$ = 0.678 ± 0.033, R^2 = 0.979, $F_{(1,9)}$ = 416.6, ***p < 0.001). We also compared the linear regressions among groups using ANCOVA. The difference between control vs Tg + **5i** was significant at the level of intercepts [ANCOVA: $F_{(1,19)}$ = 41.78, ***p < 0.001]; we also found significant differences at the level of intercepts between control and Tg + **5c** [ANCOVA: $F_{(1,19)}$ = 44.86, ***p < 0.001], and no differences comparing Tg + **5i** vs Tg + **5c**. This means that, compared to control, both **5c** and **5i** add more strength to the synaptic transmission.

Figure 12F: The three curves are not significantly different of each other (one-way ANOVA, followed by Bonferroni's post hoc test: p = 0.25).

Figure 12G: The FV amplitude values at the Tg Control and Tg + **5i** were similar, and both different from the third group (Tg control before TBS: 0.588 ± 0.004, after TBS: 0.602 ± 0.001 mV; Tg + **5i** before TBS: 0.589 ± 0.003, after TBS: 0.586 ± 0.001 mV; Tg + **5c** before TBS: 0.325 ± 0.003, after TBS: 0.354 ± 0.002 mV; one-way ANOVA ***p < 0.001, followed by Bonferroni's post-hoc test Tg control vs Tg + **5i**, p = 0.541; Tg control vs Tg + **5c**, ***p < 0.001; Tg + **5i** vs Tg + **5c** ***p < 0.001). Like for young treated animals, we first found the Pearson's correlation to obtain the correlation coefficient 'r' of each group, before the induction of LTP (Tg control: r = 0.587; Tg + **5i**: r = 0.589; Tg + **5c**: r = 0.766). We used Fisher 'r' to 'z' transformation to compute how different was the comparison between two correlation coefficients using the 'z' scores of each group (Tg control vs Tg + **5i**: z = –0.02, two-tailed p = 0.984; Tg control vs Tg + **5c**: z = –1.8, two-tailed p = 0.066; Tg + **5i** vs Tg + **5c**: z = –1.79, two-tailed p = 0.069). The negative 'z' indicates that the 'r' of the first group is smaller than the one to which is compared. Thus, compounds **5i** and **5c** make the parameters more correlated compared to the control, but not significant. Then, we obtained the correlation

coefficient ‘r’ of each group after the induction of LTP (Tg control: r = 0.489; Tg + **5i**: r = 0.669; Tg + **5c**: r = 0.539), and the ‘z’ scores of each comparison (Tg control vs Tg + **5i**: z = –3.05, two-tailed **p < 0.01; Tg control vs Tg + **5c**: z = –0.76, two-tailed p = 0.472; Tg + **5i** vs Tg + **5c**: z = 2.29, two-tailed p = 0.023). This indicates that after LTP induction, **5i** treatment turns variables more correlated than control and **5c** treatment.

Appendix (elemental analysis data)

Compound	Molecular Formula	Calculated			Found		
		C	H	N	C	H	N
5a·HCl·3/4H_2O	$C_{30}H_{34}ClN_3O_3$·HCl·3/4H_2O	63.21	6.45	7.37	63.28	6.67	7.17
5b·HCl·1/2H_2O	$C_{31}H_{36}ClN_3O_3$·HCl·1/2H_2O	64.24	6.61	7.25	64.25	6.88	7.01
5c·HCl·3/4H_2O	$C_{32}H_{38}ClN_3O_3$·HCl·3/4H_2O	64.26	6.83	7.03	64.47	7.04	6.86
5d·HCl·1/2H_2O	$C_{33}H_{40}ClN_3O_3$·HCl·1/2H_2O	65.23	6.97	6.92	65.33	7.17	6.69
5e·HCl·3/4H_2O	$C_{34}H_{42}ClN_3O_3$·HCl·3/4H_2O	65.22	7.16	6.71	65.16	7.32	6.38
5f·HCl·1.5H_2O	$C_{33}H_{32}ClN_3O_3$·HCl·1.5H_2O	64.18	5.88	6.80	63.87	5.76	6.64
5g·HCl·2H_2O	$C_{33}H_{38}ClN_3O_3$·HCl·2H_2O	62.65	6.85	6.64	62.75	6.35	6.81
5h·HCl·1/2H_2O	$C_{35}H_{42}ClN_3O_3$·HCl·1/2H_2O	66.34	7.00	6.63	66.18	7.06	6.33

5-[(3-Chloro-6,7,10,11-tetrahydro-9-methyl-7,11-methanocycloocta[*b*]quinolin-12-yl)amino]-*N*-(4-hydroxy-3-methoxybenzyl)pentanamide (**5a**)

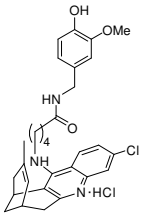

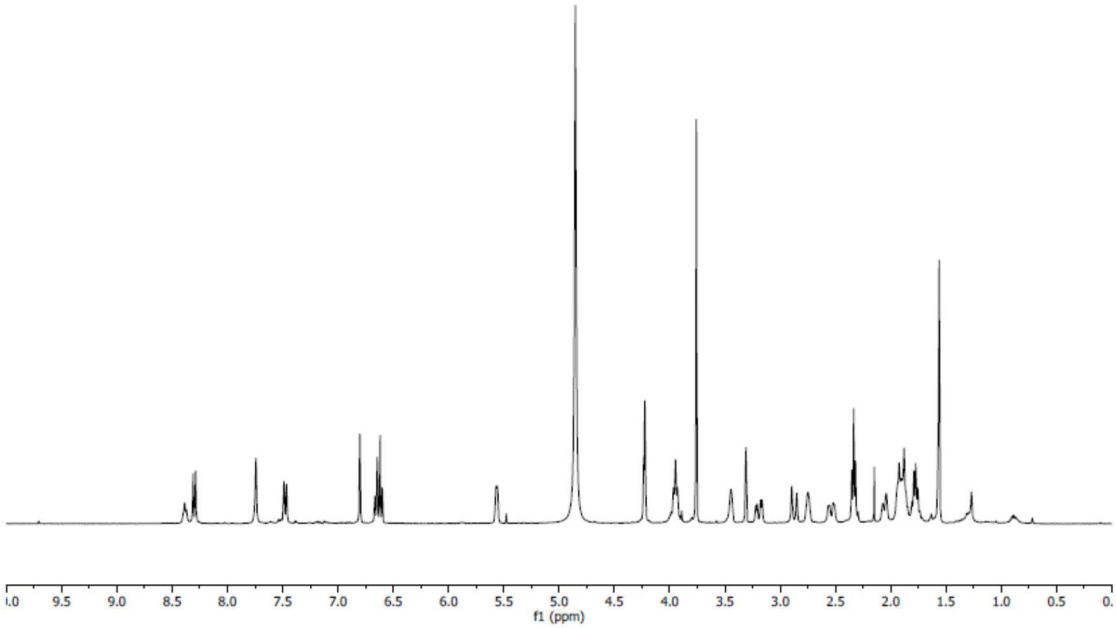

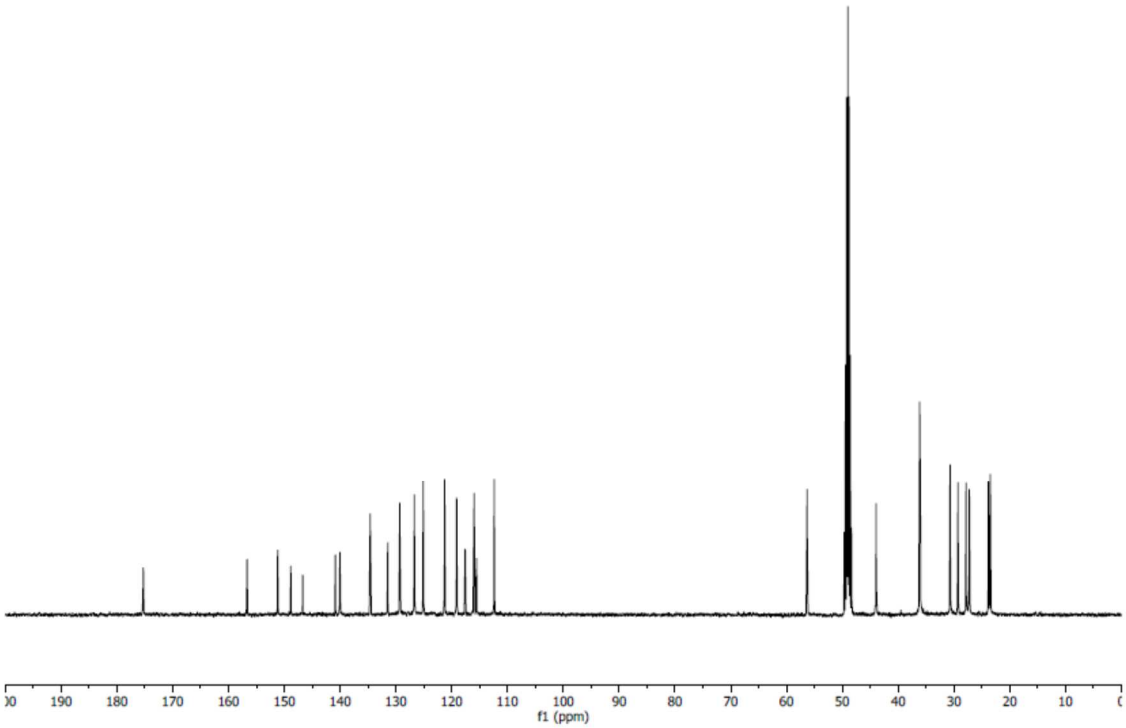

6-[(3-Chloro-6,7,10,11-tetrahydro-9-methyl-7,11-methanocycloocta[*b*]quinolin-12-yl)amino]-*N*-(4-hydroxy-3-methoxybenzyl)hexanamide (**5b**)

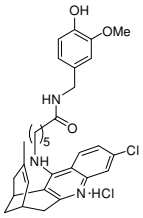

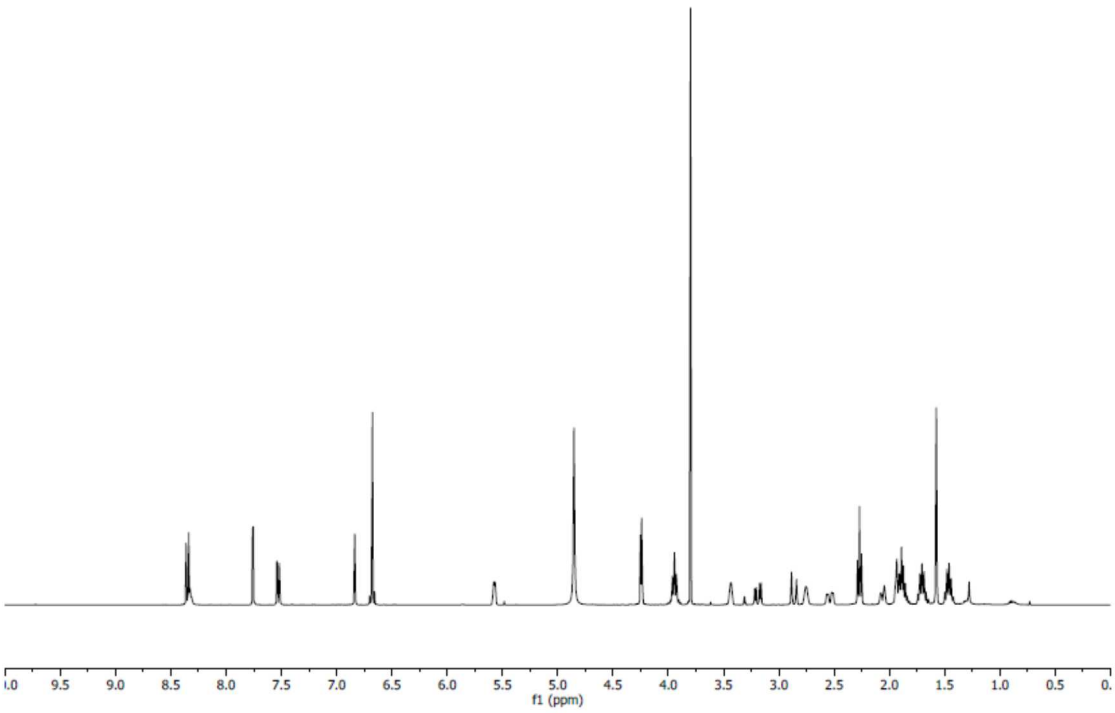

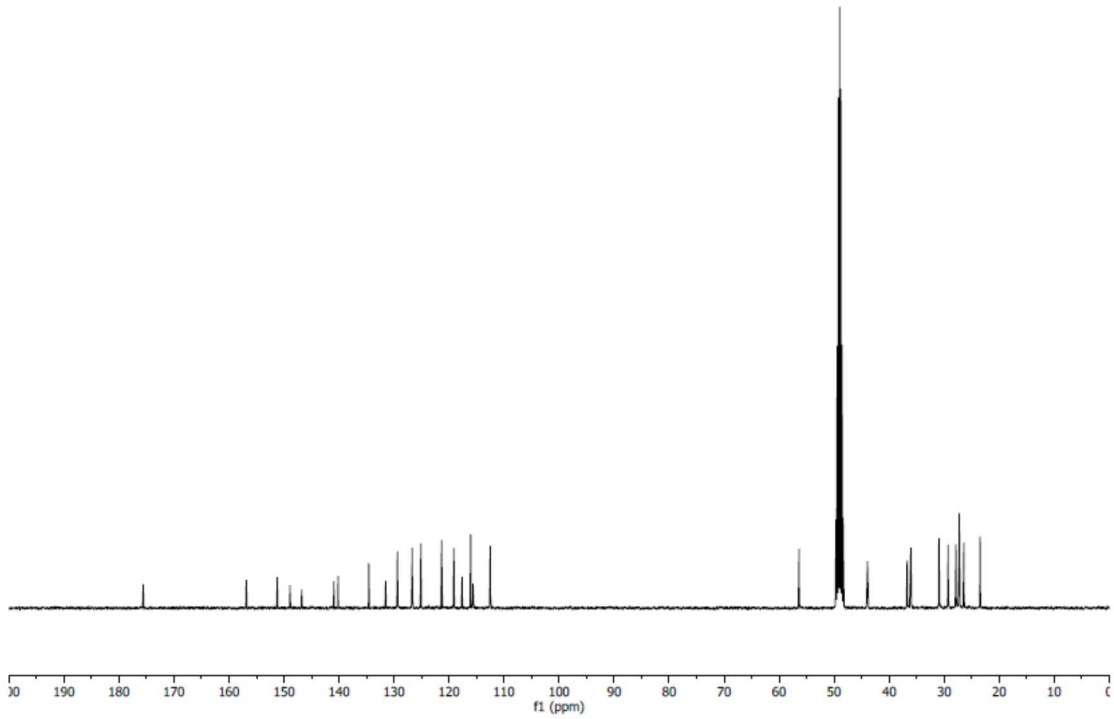

7-[(3-Chloro-6,7,10,11-tetrahydro-9-methyl-7,11-methanocycloocta[*b*]quinolin-12-yl)amino]-*N*-(4-hydroxy-3-methoxybenzyl)heptanamide (**5c**)

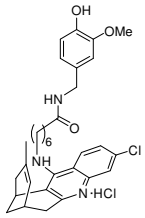

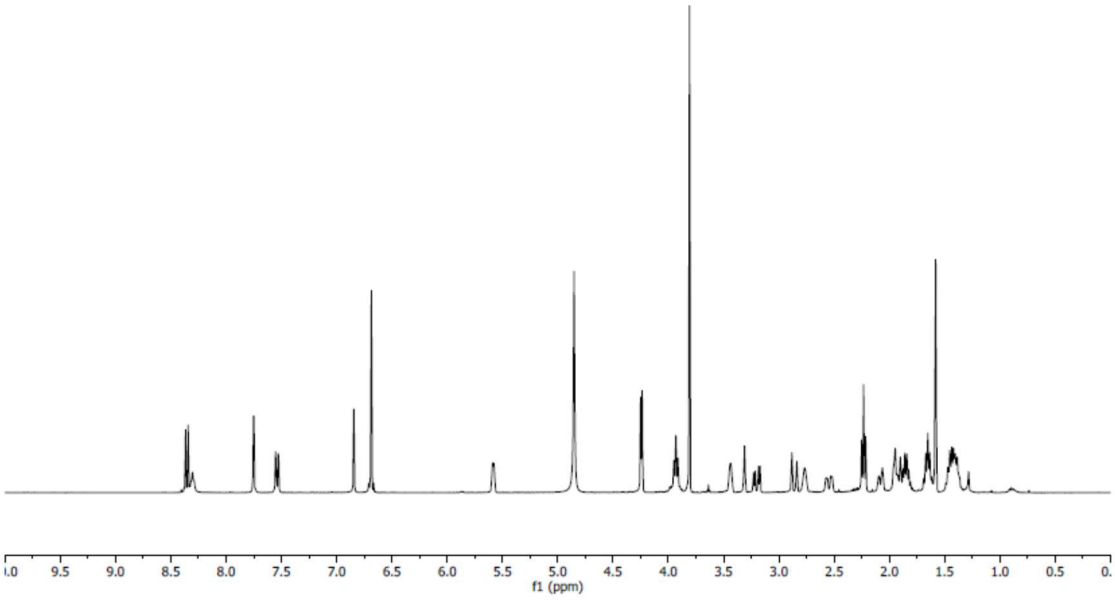

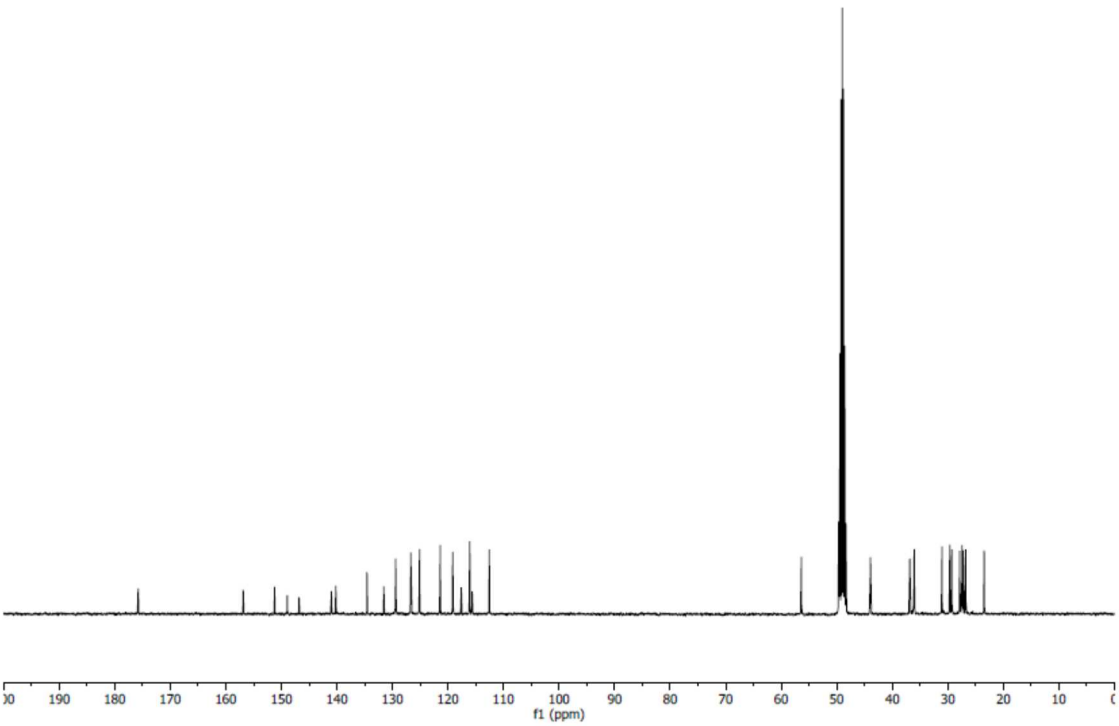

8-[(3-Chloro-6,7,10,11-tetrahydro-9-methyl-7,11-methanocycloocta[*b*]quinolin-12-yl)amino]-*N*-(4-hydroxy-3-methoxybenzyl)octanamide (**5d**)

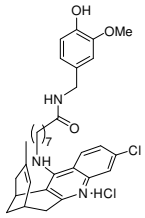

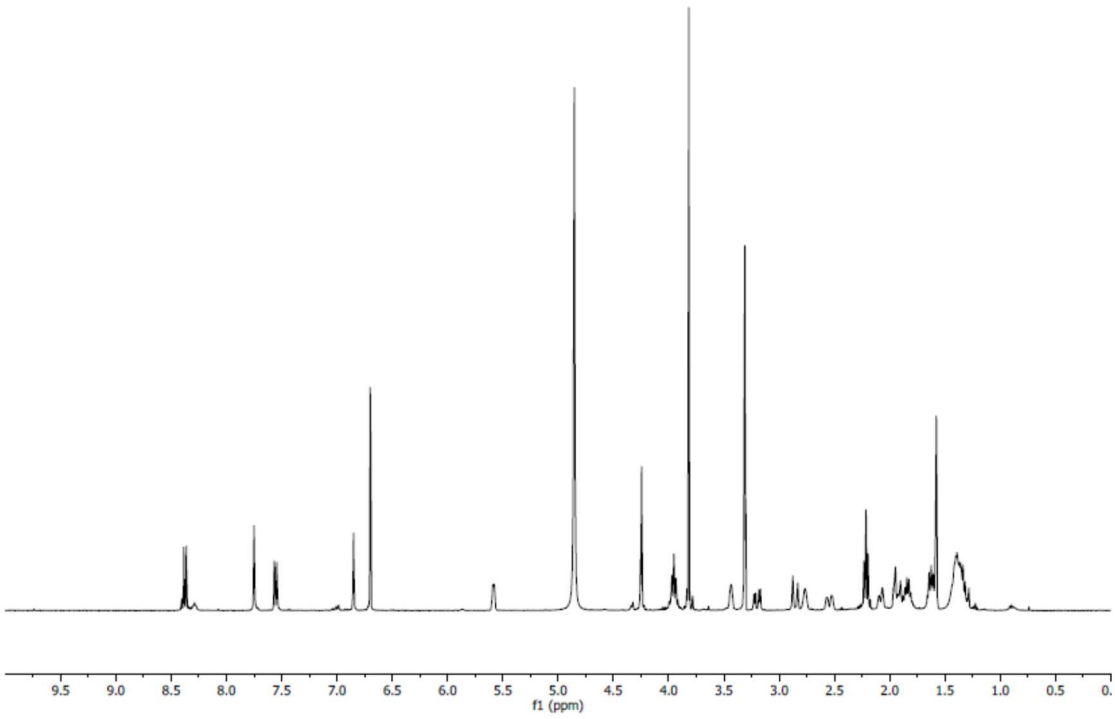

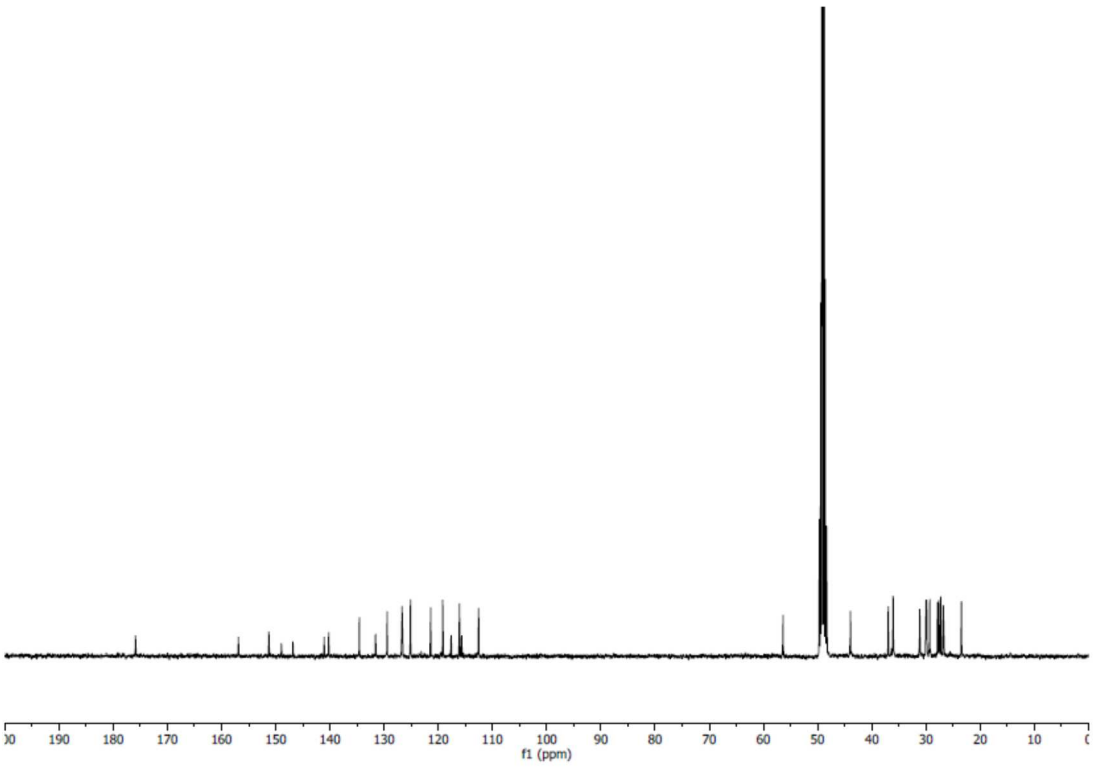

9-[(3-Chloro-6,7,10,11-tetrahydro-9-methyl-7,11-methanocycloocta[*b*]quinolin-12-yl)amino]-*N*-(4-hydroxy-3-methoxybenzyl)nonanamide (5e)

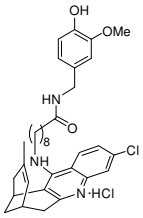

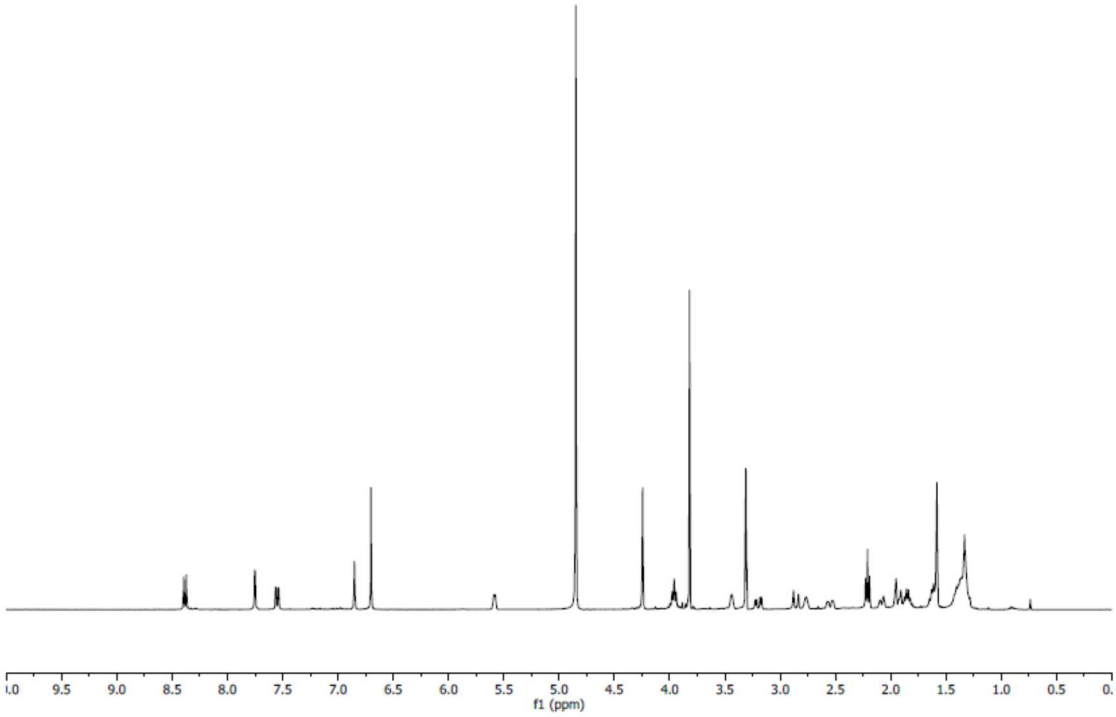

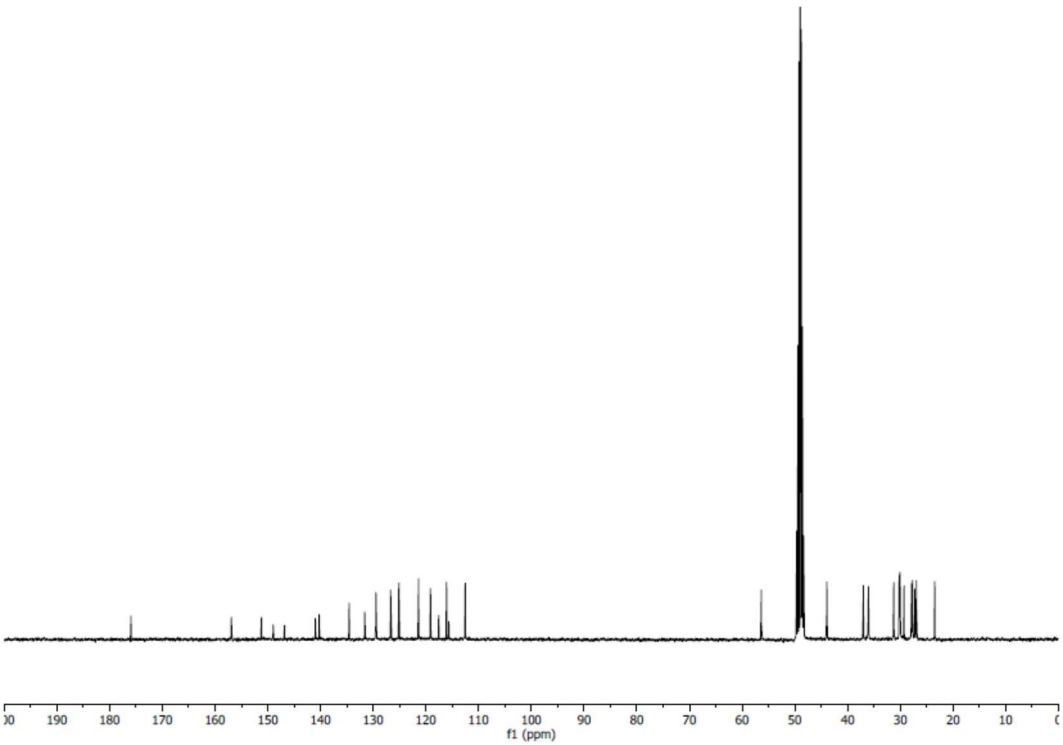

4-{[(3-Chloro-6,7,10,11-tetrahydro-9-methyl-7,11-methanocycloocta[*b*]quinolin-12-yl)amino]methyl}-*N*-(4-hydroxy-3-methoxybenzyl)benzamide (5f)

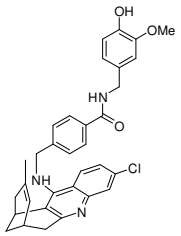

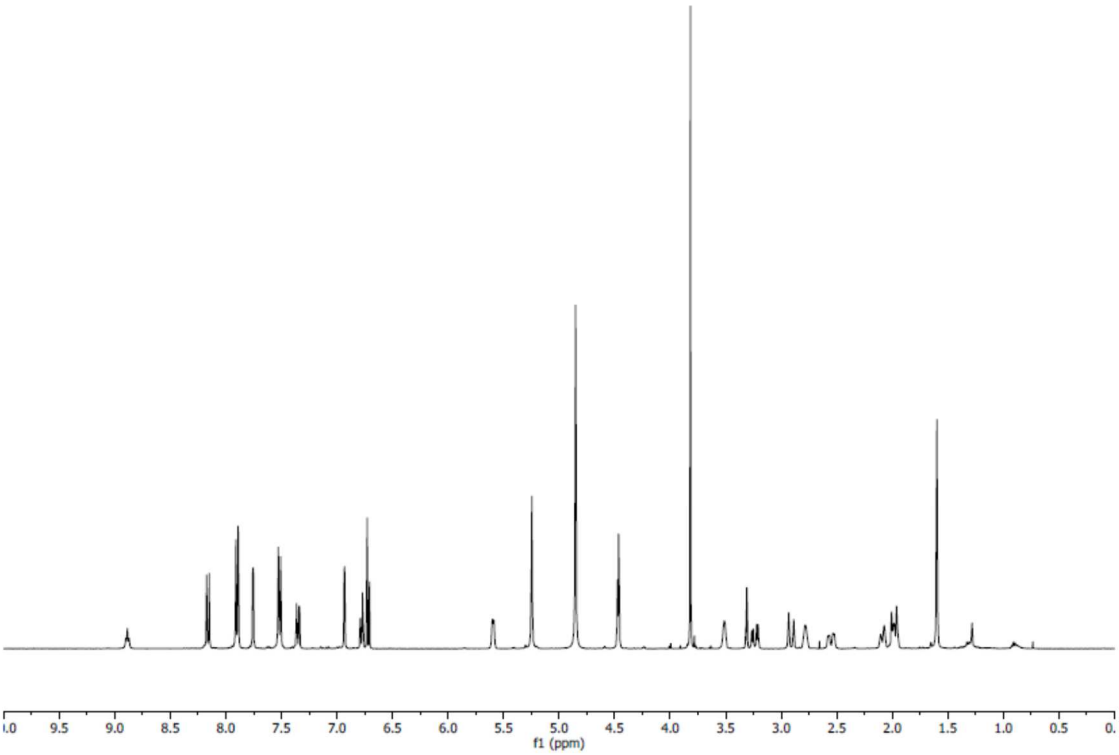

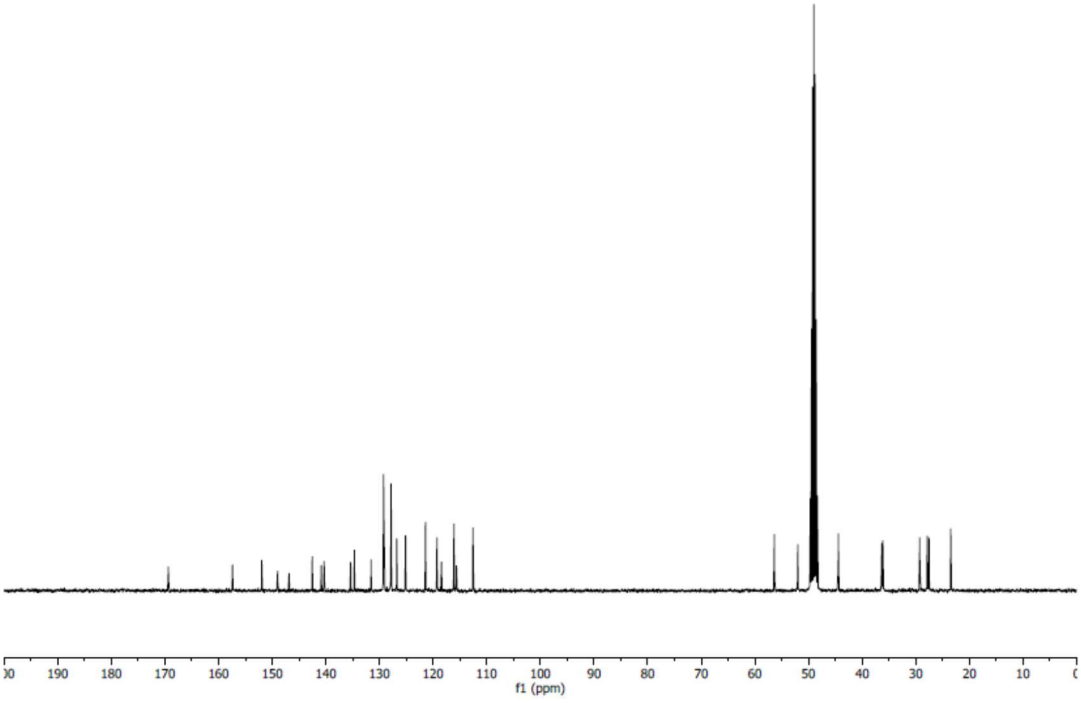

(*E*)-8-[(3-Chloro-6,7,10,11-tetrahydro-9-methyl-7,11-methanocycloocta[*b*]quinolin-12-yl)amino]-*N*-(4-hydroxy-3-methoxybenzyl)-6-octenamide (5g)

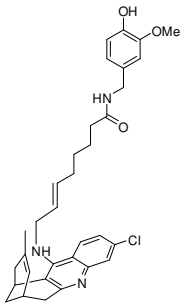

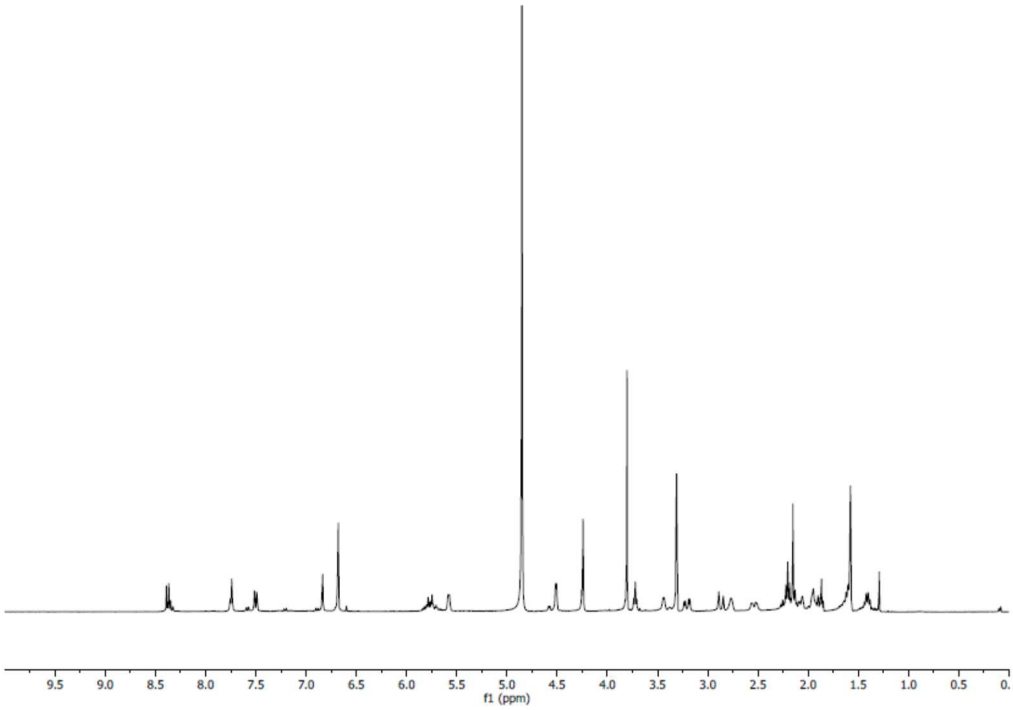

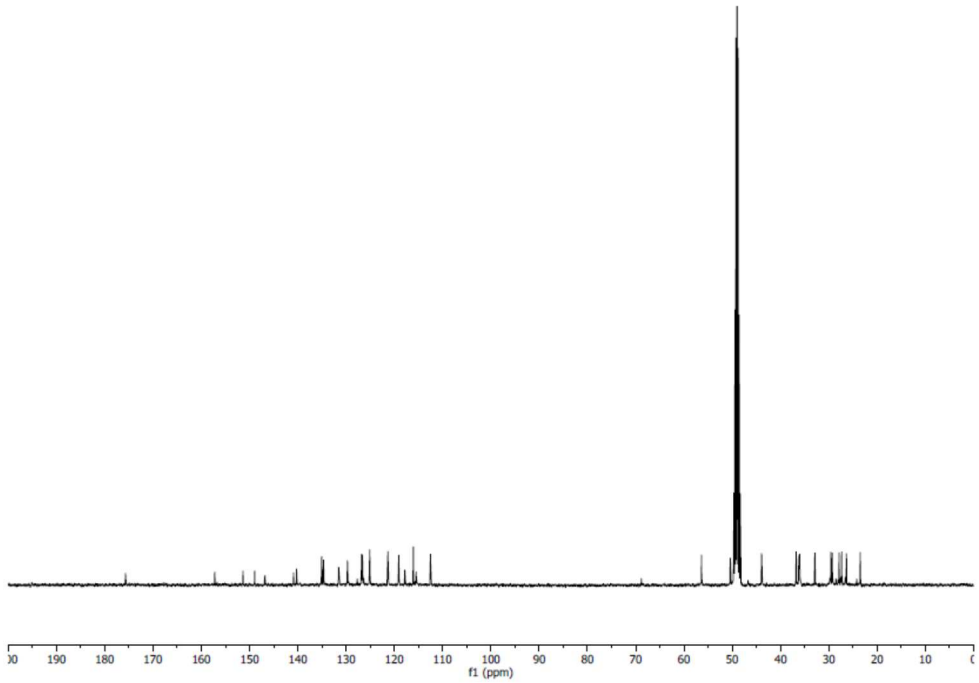

(*E*)-10-[(3-Chloro-6,7,10,11-tetrahydro-9-methyl-7,11-methanocycloocta[*b*] quinolin-12-yl)amino]-*N*-(4-hydroxy-3-methoxybenzyl)-6-decenamide (5h)

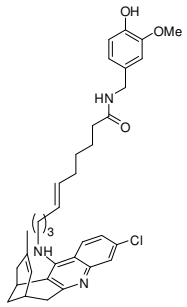

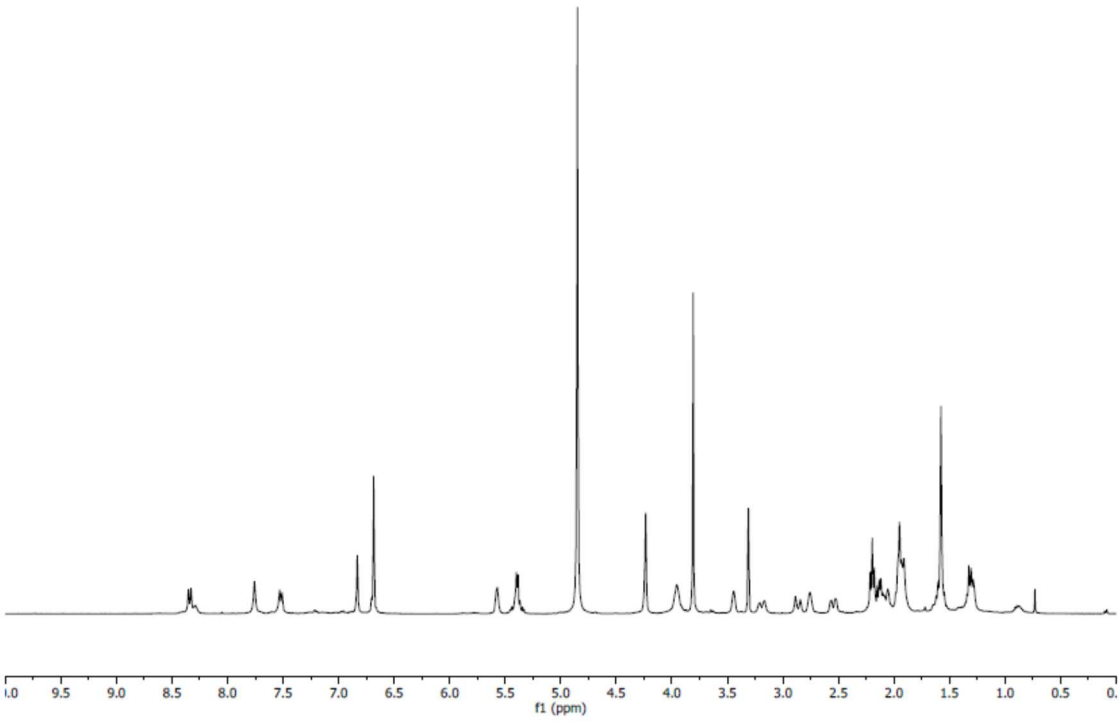

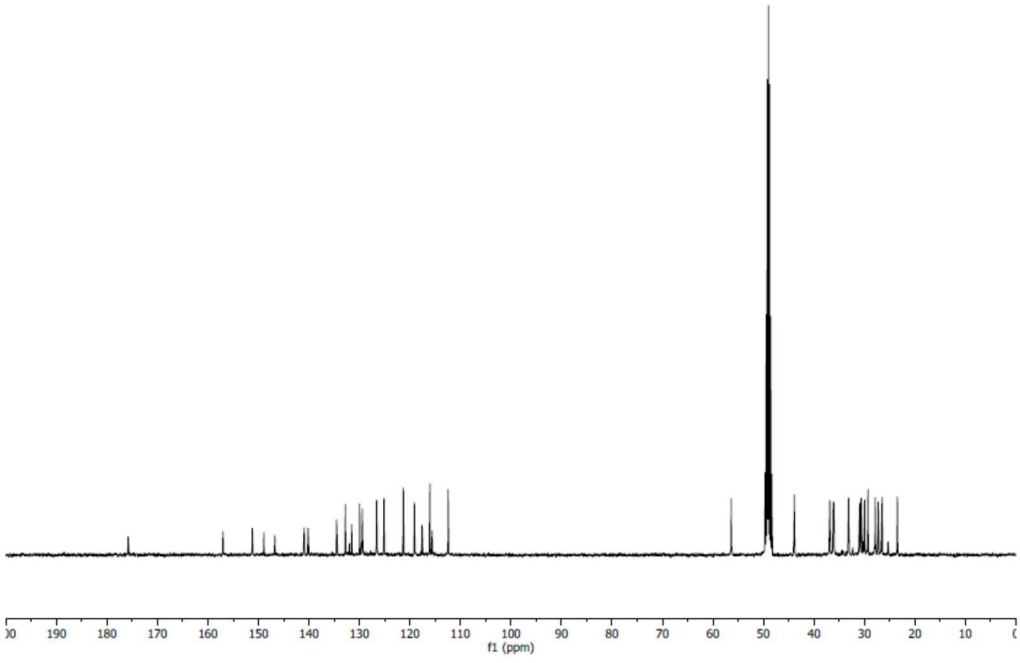

2-{1-[4-(12-Amino-3-chloro-6,7,10,11-tetrahydro-7,11-methanocycloocta[*b*]quinolin-9-yl)butyl]-1*H*-1,2,3-triazol-4-yl}-*N*-[4-hydroxy-3-methoxybenzyl]acetamide (5i)

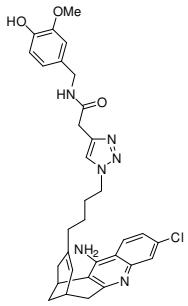

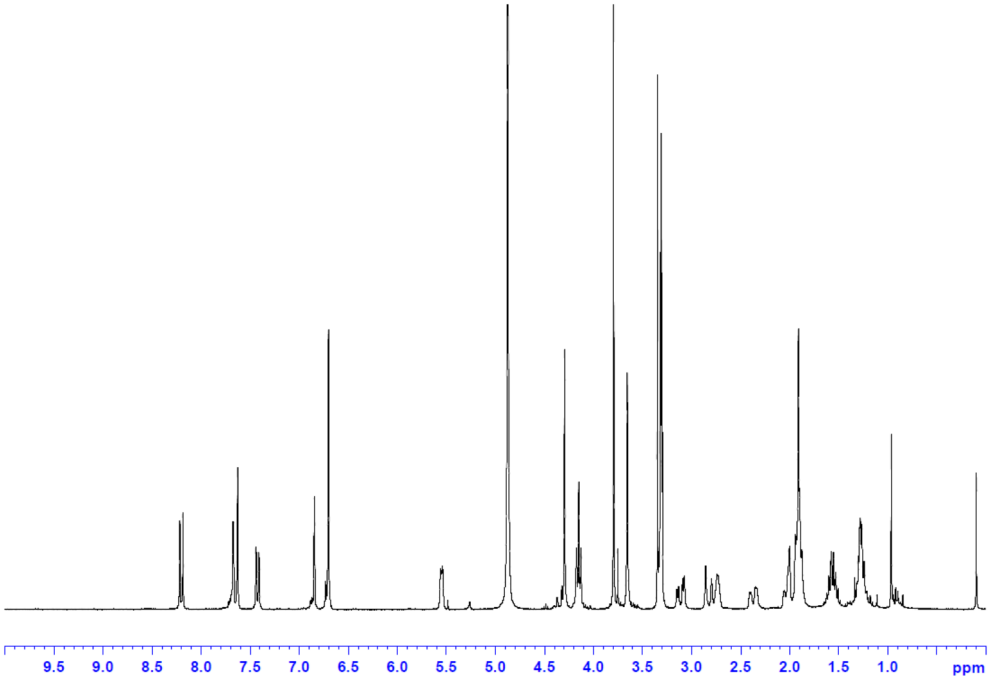

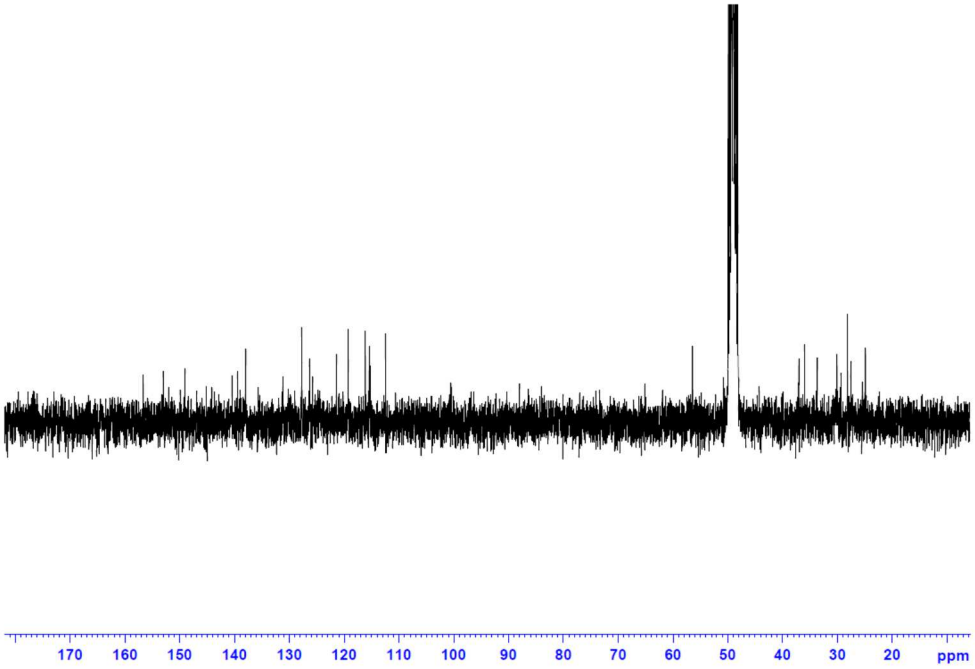

Chromatogram

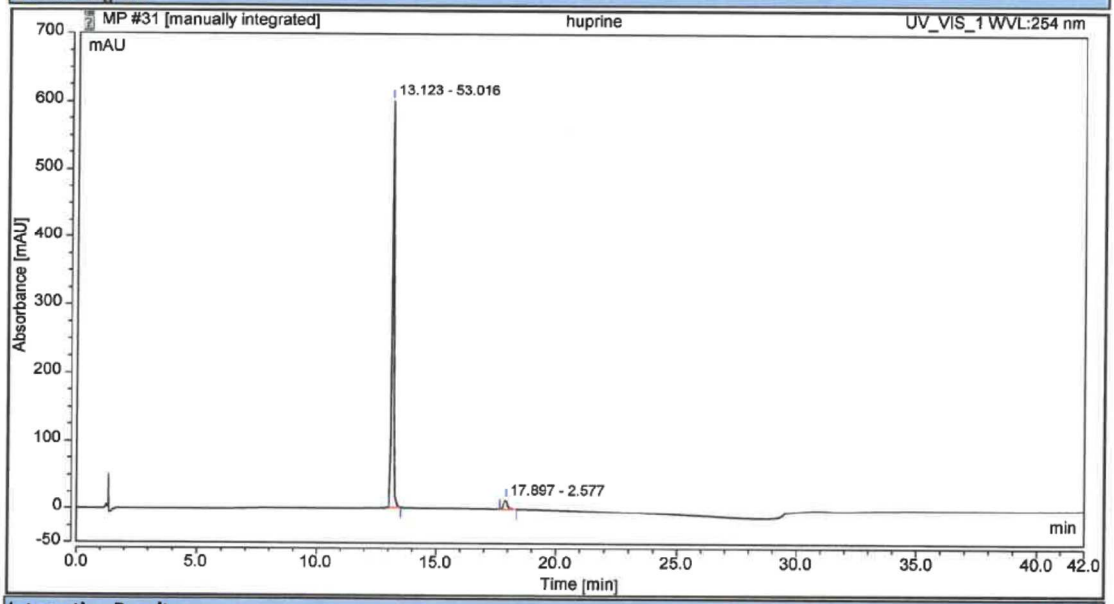

Integration Results

No.	Peak Name	Retention Time min	Area mAU*min	Height mAU	Relative Area %	Relative Height %	Amount n.a.
1		13.123	53.016	599.463	95.36	97.89	n.a.
2		17.897	2.577	12.944	4.64	2.11	n.a.
Total:			**55.593**	**612.407**	**100.00**	**100.00**	